

Sound attenuation in finite-temperature stable glasses

Lijin Wang,¹ Elijah Flenner,² and Grzegorz Szamel²

¹*School of Physics and Materials Science, Anhui University, Hefei 230601, P. R. China.*

²*Department of Chemistry, Colorado State University, Fort Collins, Colorado 80523, USA*

(Dated: November 3, 2021)

The temperature dependence of the thermal conductivity of amorphous solids is markedly different from that of their crystalline counterparts, but exhibits universal behaviour. Sound attenuation is believed to be related to this universal behaviour. Recent computer simulations demonstrated that in the harmonic approximation sound attenuation Γ obeys quartic, Rayleigh scattering scaling for small wavevectors k and quadratic scaling for wavevectors above the Ioffe-Regel limit. However, simulations and experiments do not provide a clear picture of what to expect at finite temperatures where anharmonic effects become relevant. Here we study sound attenuation at finite temperatures for model glasses of various stability, from unstable glasses that exhibit rapid aging to glasses whose stability is equal to those created in laboratory experiments. We find several scaling laws depending on the temperature and stability of the glass. First, we find the large wavevector quadratic scaling to be unchanged at all temperatures. Second, we find that at small wavevectors $\Gamma \sim k^{1.5}$ for an aging glass, but $\Gamma \sim k^2$ when the glass does not age on the timescale of the calculation. For our most stable glass, we find that $\Gamma \sim k^2$ at small wavevectors, then a crossover to Rayleigh scattering scaling $\Gamma \sim k^4$, followed by another crossover to the quadratic scaling at large wavevectors. Our computational observation of this quadratic behavior reconciles simulation, theory and experiment, and will advance the understanding of the temperature dependence of thermal conductivity of glasses.

I. INTRODUCTION

Glasses exhibit universal low-temperature thermal properties that differ markedly from those of their crystalline counterparts¹⁻³. For instance, the thermal conductivity of glasses for temperatures T below approximately 1K increases as T^2 instead of T^3 as for crystalline solids². Additionally, there is a plateau in the thermal conductivity of glasses around 10K that is absent in crystalline solids. While the two-level tunneling model²⁻⁸ predicts the T^2 increase of the thermal conductivity of glasses, there needs to be another effect to account for the ~ 10 K plateau. Zeller *et al.*³ argued that two-level tunneling combined with sound waves where sound attenuation Γ obeys Rayleigh scattering scaling, $\Gamma \sim k^4$, at small wavevector k correctly predict the low temperature T^2 and the plateau of the thermal conductivity. However, their calculation did not provide direct evidence of small wavevector Rayleigh scattering scaling of sound attenuation.

Scattering experiments were able to provide direct evidence for the existence of Rayleigh scattering scaling at low temperatures⁹⁻¹⁵, and how anharmonicity modifies sound attenuation at finite temperatures¹². Baldi *et al.*¹² used inelastic x-ray scattering to demonstrate that the small wavevector, low temperature sound attenuation obeys Rayleigh scattering scaling for a network glass former. However, they also found that at higher temperatures sound attenuation scales quadratically with wavevector at small wavevectors and at large wavevectors with a quartic, Rayleigh scattering scaling region in between. The small wavevector quadratic scaling was strongly temperature dependent, while the large wavevector quadratic scaling was nearly tempera-

ture independent. Other scattering studies support the picture that anharmonic effects give rise to $\Gamma \sim k^2$ for both small and large wavevectors for most glass formers¹⁶⁻¹⁹. The small wavevector quadratic scaling has been attributed to damping due to a spatial variation of the strain field leading to heat flow (thermoelastic dissipation)²⁰⁻²², heat flow between different sound modes (Akhiezer damping)^{23,24}, and to spatial fluctuations of the elastic constants (fluctuating elasticity)²⁵.

Surprisingly, it was found in vitreous germanium that sound attenuation increased linearly with frequency at small frequencies²⁶, implying a linear instead of quadratic increase of sound attenuation with wavevector and non-universal behavior. Fluctuating elasticity theory predicts that anharmonic effects results in non-quadratic scaling of sound attenuation at small wavevectors close to an elastic instability²⁷, and a quadratic scaling of sound attenuation sufficiently far from an elastic instability²⁸. Additionally, fluctuating elasticity theory predicts that the harmonic quartic scaling at small wavevectors is observable at low enough temperatures²⁸. While fluctuating elasticity theory correctly describes sound attenuation qualitatively, it has recently been shown to fail quantitatively²⁹.

Recently, large-scale computer simulations confirmed Rayleigh scattering scaling of sound attenuation in the harmonic approximation at small wavevectors and quadratic scaling at large wavevectors³⁰⁻³². It is not expected that the quadratic small wavevector scaling could be captured in the harmonic approximation since this scaling is attributed to anharmonic effects. Between the small wavevector quartic and large wavevector quadratic regime a possible crossover $k^4 \ln(k)$ regime has been identified in simulations²⁹⁻³³, but this crossover

region shrinks with increasing glass stability³². To observe Rayleigh scattering scaling in simulations researchers have to utilize very large systems³⁰ or examine very stable glasses³². These stable simulated glasses have only recently become available due to the combination of the swap algorithm and model polydisperse glass formers^{34,35}. The Rayleigh scattering scaling regime extends to larger wavevectors as the stability of the glass increases, and thus smaller systems can be simulated to clearly observe Rayleigh scattering scaling³².

Simulations have not provided a clear picture of the temperature dependence of sound attenuation in model glass formers. Busselez, Pezeril, and Gusev³⁶ used molecular dynamics simulations to examine the sound attenuation in a model of glycerol. For small frequencies, they reported quadratic scaling of sound attenuation with frequency at intermediate temperatures and cubic scaling with frequency at lower temperatures. They did not clearly see the three regimes observed in the experiments of Baldi *et al.*¹², the low and high frequency quadratic scaling and the intermediate quartic scaling. Mizuno and Mossa recently studied glasses obtained by rapidly quenching a mono-disperse Lennard-Jones fluid^{37,38}, and found results consistent with fluctuating elasticity theory close to an elastic instability²⁷. Specifically, at a finite temperature below the glass transition temperature but high enough for anharmonic effects to be present, Mizuno and Mossa found that $\Gamma \sim k^{1.5}$ at small wavevectors, $\Gamma \sim k^2$ at large wavevectors, and an intermediate quartic regime, $\Gamma \sim k^4$.

The collection of these results leaves an unclear picture of the small wavevector sound attenuation in finite temperature amorphous solids. Here we are able to help clarify the picture by studying the temperature dependence of sound attenuation in poorly annealed glasses and in extremely stable glasses. The stability of our stable glasses is comparable to that of exceptionally stable laboratory glasses created using vapor deposition^{39,40}. We observe nearly all the scaling behavior reported in the experiments and simulations discussed above. For our poorly annealed glasses, we find that $\Gamma \sim k^{1.5}$ at small wavevectors while the glass is undergoing aging on the time scale of the simulation. The evidence for aging comes from an upturn in the mean-square-displacement. For glasses that are not noticeably aging on the time scale of the simulation, we find that $\Gamma \sim k^2$ at small wavevectors and large wavevectors. Between these two quadratic scaling regimes we clearly observe a quartic scaling regime in our extremely stable glasses. We characterize the temperature dependence of the different scaling regimes.

II. SIMULATION DETAILS

We simulated $N = \{48000, 96000, 192000\}$ polydisperse spheres having equal mass m with periodic boundary conditions. Particle diameters $\sigma \in [0.73, 1.63]$ have a distribution $P(\sigma) \sim \sigma^{-3}$. To prevent demixing, we em-

ploy a non-additive mixing rule to determine the cross-diameter σ_{ij} , $\sigma_{ij} = \frac{\sigma_i + \sigma_j}{2}(1 - \epsilon|\sigma_i - \sigma_j|)$ with $\epsilon = 0.2$. Particles i and j interact via the inverse power law potential $V(r_{ij}) = \left(\frac{\sigma_{ij}}{r_{ij}}\right)^{12} + V_c(r_{ij})$ when the separation between particles i and j , $r_{ij} < r_{ij}^c = 1.25\sigma_{ij}$ and $V(r_{ij}) = 0$ if $r_{ij} \geq r_{ij}^c$. Here, $V_c(r_{ij}) = c_0 + c_2 \left(\frac{r_{ij}}{\sigma_{ij}}\right)^2 + c_4 \left(\frac{r_{ij}}{\sigma_{ij}}\right)^4$ and the coefficients are chosen so that $V(r_{ij})$ and its first two derivatives are continuous at r_{ij}^c . The number density $\rho = 1.0$. For reference, the onset temperature of slow dynamics $T_o \approx 0.200$, the mode coupling temperature $T_c \approx 0.108$, and the estimated experimental glass temperature $T_g \approx 0.072$ ^{35,41}.

We obtain equilibrated supercooled liquids using the swap Monte Carlo algorithm^{34,35} at temperatures ranging from T_o down to 0.062, which is lower than T_g . To create a glass, we quench a configuration equilibrated at a temperature T_p , which we call the parent temperature of this glass, to its inherent structure using the fast inertial relaxation engine minimization⁴². We then heat the glass to the desired temperature T in the NVT ensemble^{43,44}. Finally, the system is equilibrated for a time referred in the following as the ageing time τ_{age} before the production runs start. The total length for the production run is equal to 4000, and we average over different initial configurations equilibrated at T_p . Thus, the finite temperature glass is characterized by three parameters $\{T, T_p, \tau_{age}\}$ and its stability is determined by a combination of T_p and τ_{age} .

We calculate sound attenuation Γ_λ from the decay of the current density correlation functions

$$C_\lambda(k, t) = \left\langle \frac{\vec{J}_\lambda(k, t) \cdot \vec{J}_\lambda(-k, 0)}{\vec{J}_\lambda(k, 0) \cdot \vec{J}_\lambda(-k, 0)} \right\rangle \quad (1)$$

with

$$\vec{J}_T(k, t) = \sum_{j=1}^N [\vec{v}_j(t) - (\vec{v}_j(t) \cdot \hat{k})\hat{k}] e^{i\vec{k} \cdot \vec{r}_j(t)} \quad (2)$$

for transverse current, T , and

$$\vec{J}_L(k, t) = \sum_{j=1}^N [(\vec{v}_j(t) \cdot \hat{k})\hat{k}] e^{i\vec{k} \cdot \vec{r}_j(t)} \quad (3)$$

for longitudinal current, L . Here, $\vec{v}_j(t)$ is the velocity of particle j at time t , $k = |\vec{k}|$, $\hat{k} = \vec{k}/|\vec{k}|$ with \vec{k} the wavevector.

Previous studies demonstrated either explicitly^{31,32} or implicitly⁴⁵ that there are finite size effects in the calculations of sound attenuation within the harmonic approximation. We find the finite-size effects persist for finite temperatures, especially at low temperatures. Shown in Fig. 1(a), are $C_T(k, t)$ at nearly the same wavevector but for two different system sizes. They overlap and decay exponentially at short times, but then deviate at longer times.

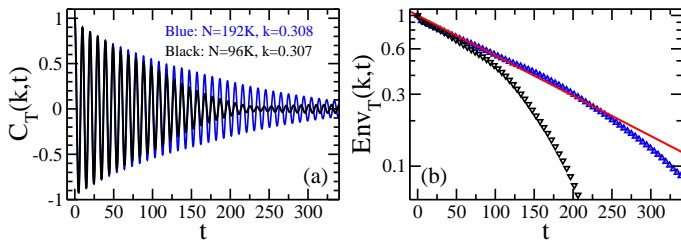


FIG. 1: Transverse current correlation functions $C_T(k, t)$ in the left panel, (a), and their corresponding envelopes $\text{Env}_T(k, t)$ in the right panel, (b), for two system sizes, $N = 96K$ (black) and $192K$ (blue), at a similar magnitude of the wavevector $k \approx 0.31$. The solid line in (b) represents a fit to $\exp(-\Gamma t/2)$. The fit works well up to longer times in $N = 192K$ system.

To eliminate finite size effects, we use a restricted envelope fit method as described in detail by Wang *et al.*³². We determine Γ_λ by fitting the envelope of $C_\lambda(k, t)$ to $\exp(-\Gamma_\lambda t/2)$ up to the time when the envelope starts to significantly deviate from exponential decay. Shown in Fig. 1(b) is the envelope of $C_T(k, t)$ shown in Fig. 1(a) and a fit to the larger system. Fits to the exponentially decaying part give the same sound attenuation within error. Therefore, in this work sound attenuation combined from different system sizes is shown without distinguishing system sizes since finite size effects have been removed.

III. TEMPERATURE DEPENDENCE OF SOUND ATTENUATION IN STABLE GLASSES

We examined the finite-temperature sound attenuation in our most stable glasses with parent temperature $T_p = 0.062$. The stability of these model stable glasses has been demonstrated by Ninarello *et al.*³⁵ to be comparable to that of experimental glasses, which makes the present study of sound attenuations relevant for experimental glasses. We find that sound attenuation in stable glasses at temperatures below $T_g \approx 0.072$ shows no τ_{age} dependence in any of our simulations. We aged the systems up to τ_{age} equal to one million.

Shown in Fig. 2 is the temperature dependence of the transverse (a) and longitudinal (b) sound attenuation in our most stable glasses. The small wavevector quadratic behaviour for Γ_λ can be observed at all temperatures, except for Γ_L at $T = 0.001$, Fig. 2(b). At small k , we expect that $\Gamma_L(k) \sim k^2$ at $T = 0.001$ if we can simulate a much larger system. At large wavevectors, we find a temperature independent, quadratic dependence of Γ_λ on wavevector that is different from the small wavevector quadratic dependence. Rayleigh scattering scaling is found between the large wavevector and small wavevector quadratic regimes. The coefficients quantifying sound attenuation in the Rayleigh scattering regime, Γ_λ/k^4 , are approximately temperature-independent. We con-

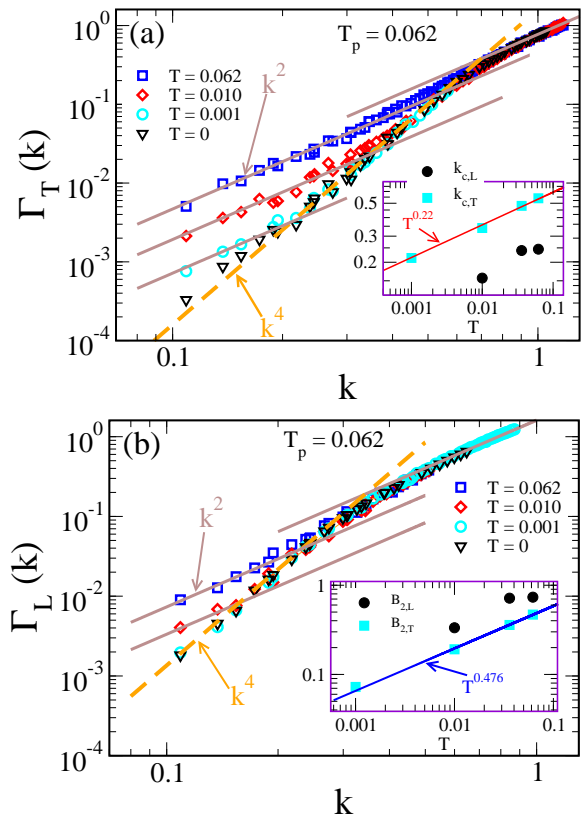


FIG. 2: Wavevector k dependence of transverse sound attenuation $\Gamma_T(k)$ (a) and longitudinal sound attenuation $\Gamma_L(k)$ (b) for our most stable glass, $T_p = 0.062$ at different temperatures T . The aging time $\tau_{\text{age}} = 1000$, but these results are independent of the aging time. The inset in (a) shows the T dependent upper wavevector $k_{c,T}$ and $k_{c,L}$ for the low- k quadratic scaling. $k_{c,\lambda}$ at each T is roughly defined as the crossover between the low- k quadratic law (solid line) and the intermediate- k quartic law (dashed line) in (a) and (b). The solid line in the inset is a fit of $k_{c,T}$ to $T^{0.22}$. The inset in (b) shows the T dependence of the low- k quadratic coefficients $B_{2,T}$ and $B_{2,L}$, *i.e.* $\Gamma_T(k) = B_{2,T}k^2$ and $\Gamma_L(k) = B_{2,L}k^2$. The solid line in the inset indicates a fit of $B_{2,T}$ to $T^{0.476}$.

clude that the finite temperature anharmonic effects alter sound attenuation predominately at small wavevectors.

These results mirror the results reported in the experiments of Baldi *et al.*¹², who also reported Rayleigh scattering scaling for low temperatures and quadratic scaling at small wavevector with increasing temperature. To analyze their results, Baldi *et al.* fit the sound attenuation to a model that included an Akhieser term and a Rayleigh scattering scaling term. Future work needs to examine if a similar model is reasonable for model glass formers, but this is outside the scope of this study.

Next, we examine the temperature dependence of small-wavevector quadratic scaling of sound attenuation. First, we study the temperature dependence of the largest wavevector, $k_{c,\lambda}$ where $\Gamma_\lambda(k)$ scales quadratically, see the inset to Fig. 2(a). We define $k_{c,\lambda}$ as the intersection of the small- k quadratic and intermediate- k quartic

fitting lines. At all temperatures, $k_{c,T}$ is found to be larger than $k_{c,L}$, and thus, if a characteristic length scale determines this crossover, this length scale must be different for longitudinal and transverse sound. Moreover, as T increases, both $k_{c,T}$ and $k_{c,L}$ increase. We find that a power law $k_{c,T} \sim T^{0.22}$ describes well the temperature dependence of $k_{c,T}$. Given the uncertainties in our determination of $k_{c,T}$ and the limited range of $k_{c,T}$, we do not exclude the possibility that the temperature dependence of $k_{c,T}$ can be described by other functions. Our fit suggests that we would need an approximately 1 million particle system to observe the small wavevector quadratic scaling for longitudinal attenuation at $T = 0.001$ for the parent temperature $T_p = 0.062$.

The temperature dependence of the small wavevector quadratic coefficients, $B_{2,\lambda} = \Gamma_\lambda(k)/k^2$ is shown in the inset to Fig. 2(b). Both $B_{2,T}$ and $B_{2,L}$ increase with increasing T , and thus the small wavevector sound attenuation becomes progressively stronger with increasing temperature. We also find $B_{2,T}(T)$ is always smaller than $B_{2,L}(T)$, hence the longitudinal sound attenuation is larger than the transverse wave attenuation at a fixed wavevector. This observation is consistent with the conclusion in the study of sound attenuation within the harmonic approximation³². Moreover, $B_{2,T}(T)$ can be fitted well with a power law, $B_{2,T}(T) \sim T^\beta$ with $\beta = 0.476 \pm 0.015$. This value of β is different than the fluctuating elasticity theory²⁵ prediction of $\beta = 1$ for a system not close to an elastic instability.

Fluctuating elasticity theory²⁷ predicts that $\Gamma_T = B_{1.5,T}k^{1.5}$ with $B_{1.5,T} \sim T^{0.5}$ close to an elastic instability. While the temperature scaling exponent is close to the value we get from our fits, the small wavevector scaling is different, and thus the theory is not consistent with our results. Mizuno and Mossa^{37,38} obtained results consistent with fluctuating elasticity theory for a mono-disperse Lennard-Jones glass, which is a poor glass former that is prone to crystallization. We do not observe the $k^{1.5}$ scaling for small wavevectors for our stable glasses, but we observe this scaling for an aging glass, which is described in Section IV. More work is needed to disentangle the similarity and difference observed here between our simulations and existing theoretical predictions.

Previous simulation studies^{32,46} of sound attenuation within the harmonic approximation demonstrated that for a fixed stability, when attenuation is examined as a function of frequency, the scaling behavior for longitudinal and transverse attenuation is the same, *i.e.* the frequency dependent longitudinal and the transverse attenuation overlap when scaled by a constant factor. We find that this also holds at finite temperatures, and $\Gamma_T(\omega) = S * \Gamma_L(\omega)$ where $S \approx 3$ if when we use speeds of sound to replace the wavevector by the frequency, $\omega = v_\lambda k$ where v_λ is the speed of sound, Fig. 3. If we obtain ω directly from the fits to $C_\lambda(k, t)$ we find $S \approx 3.5$, but the scaling still holds. At small ω , we find $\Gamma_T(\omega) \sim \omega^2$ for all temperatures including $T = 0.001$.

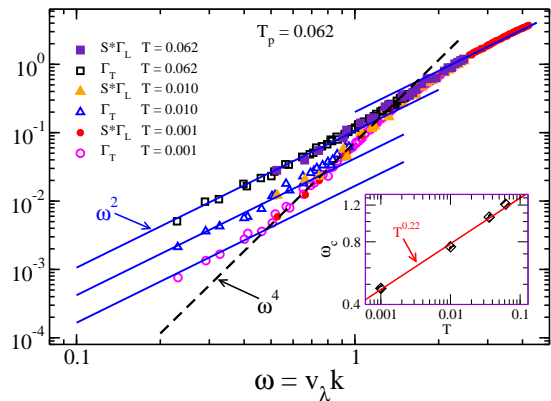


FIG. 3: Sound attenuation as a function of frequency $\omega = v_\lambda(T)k$ for glasses at $T = 0.001, 0.010$ and 0.062 , with parent temperature $T_p = 0.062$ and waiting time $\tau_{\text{age}} = 1000$. The values of v_T (v_L) for $T = 0.001, 0.010$ and 0.062 glasses are approximately 2.125 (4.838), 2.121 (4.828) and 2.109 (4.811), respectively. The longitudinal sound attenuation Γ_L for each glass is multiplied by the same factor $S \approx 3$. In the inset is the T dependence of the upper frequency ω_c for the low- ω quadratic scaling. We roughly define ω_c as the intersection of the low- ω quadratic and the intermediate- ω quartic lines indicated in the main plot.

While for $T = 0.001$ we do not observe $\Gamma_L(k) \sim k^2$ at small k , Fig. 2(b), we hypothesize that $\Gamma_L(k) \sim k^2$ would be observed at smaller wavevectors than we have available due to the frequency scaling. Additionally, since $\Gamma_T(\omega) \sim \Gamma_L(\omega)$ then the upper frequency ω_c for this quadratic scaling of $\Gamma_\lambda(\omega)$ is independent of the polarization. The same characteristic frequency can be associated with the change of scaling of both longitudinal and transverse sound attenuation. The temperature dependence of ω_c is given in the inset to Fig. 3, and we find that ω_c increases as T increases and scales approximately as $T^{0.22}$ which is the same temperature scaling as that of $k_{c,T}$.

IV. STABILITY DEPENDENCE OF SOUND ATTENUATION

We examined the stability dependence of sound attenuation. The stability of the glass can be increased by aging the glass or by changing the protocol used to prepare it. For example, the supercooled liquid can be cooled slower to create a more stable glass, or, for some glass formers, physical vapor deposition can make very stable glasses. We begin our study of the stability dependence of sound attenuation by examining sound attenuation in an aging glass, where we monitor the aging process using the mean square displacement. We only study aging effects for a poorly annealed glass. Next, we study increasingly more stable glasses by investigating the parent temperature dependence of sound attenuation.

Our poorly annealed glass, with parent temperature

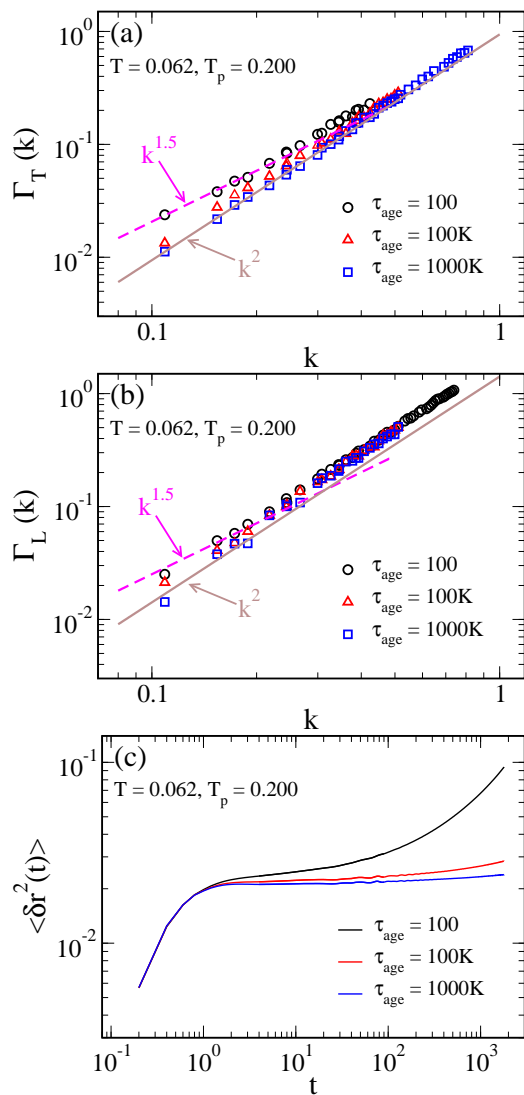


FIG. 4: Transverse sound attenuation $\Gamma_T(k)$ (a) and longitudinal sound attenuation $\Gamma_L(k)$ (b) in glasses at temperature $T = 0.062$ prepared by quenching from parent temperature $T_p = 0.200$, for aging times $\tau_{\text{age}} = \{100, 100K, 1000K\}$. The scaling of sound attenuation changes from $k^{1.5}$ when $\tau_{\text{age}} = 100$ to k^2 when $\tau_{\text{age}} = 100K$ and $1000K$. The mean-squared displacement $\langle \delta r^2(t) \rangle$ (c) depends significantly on the aging time.

$T_p = 0.2$, is prepared by quenching from the temperature corresponding to the onset of slow dynamics. The aging of this glass is clearly seen in its the mean square displacement $\langle \delta r^2(t) \rangle = N^{-1} \left\langle \sum_{j=1}^N [\vec{r}_j(t) - \vec{r}_j(0)]^2 \right\rangle$. Shown in Fig. 4(c) is $\langle \delta r^2(t) \rangle$ for the poorly annealed glass, for three aging times, $\tau_{\text{age}} = 100, 100K, 1000K$. There is a significant upturn in $\langle \delta r^2(t) \rangle$ for $\tau_{\text{age}} = 100$, but no significant upturn for the longer aging times. However, $\langle \delta r^2(t) \rangle$ depends significantly on the aging time.

We calculated $C_\lambda(k, t)$ over the time frame shown in Fig. 4(c) for the glasses with the three different aging times and determined Γ_λ from the envelope fits. Shown

in Figs. 4(a) and (b) is sound attenuation at these three aging times. With increasing τ_{age} we observe the small k scaling of $\Gamma_\lambda(k)$ changes from the $k^{1.5}$ for $\tau_{\text{age}} = 100$, for which the mean square displacement $\langle \delta r^2(t) \rangle$ exhibits a significant upturn at late times, to k^2 for the glasses with $\tau_{\text{age}} = 100K$ and $\tau_{\text{age}} = 1000K$, for which there is little to no upturn in $\langle \delta r^2(t) \rangle$. This suggests the $k^{1.5}$ scaling observed at small wavevectors in our poorly annealed glass is due to aging, and for a glass with no measurable aging, sound attenuation scales as k^2 for small wavevectors.

The $k^{1.5}$ scaling is consistent with the scaling reported by Mizuno^{37,38}, but they report that their glass is not undergoing aging. Mizuno studied a monodisperse Lennard-Jones systems, which is known to be a very poor glass former as it easily crystallizes. For this reason it may be closer to an elastic instability that is predicted to give rise to the $k^{1.5}$ scaling of sound attenuation^{26,27}. However, we find that aging can also result in $k^{1.5}$ scaling at small wavevectors.

Next we examine the stability dependence of sound attenuation by examining the parent temperature T_p dependence of sound attenuation. Here we fix $\tau_{\text{age}} = 1000$ and $T = 0.062$ while we vary T_p for glasses corresponding to poorly annealed, $T_p = 0.2$, to our most stable glass, $T_p = 0.062$. We note that τ_{age} does not statistically modify our results for $T_p \leq 0.1$ since we cannot run the molecular dynamics simulations long enough to significantly age the system.

Shown in Fig. 5(c) is $\langle \delta r^2(t) \rangle$ for $T_p = 0.2, 0.1, 0.085$, and 0.062 . There is a significant upturn for $T_p = 0.2$, but not for the other glasses. As shown previously, this upturn corresponds to $\Gamma_\lambda \sim k^{1.5}$ at small wavevectors, Figs. 5(a) and (b) for the glass created at $T_p = 0.2$. We find that for the other glasses that $\Gamma_\lambda \sim k^2$ at small wavevectors.

Recent simulation studies^{31,32} within the harmonic approximation have concluded that sound attenuation decreases with increasing glass stability. By studying sound attenuation at finite temperatures, we find the same conclusion also holds when anharmonic effects are included. This is supported by the observation that $\Gamma_\lambda(k)$ in our poorly annealed glass with $T_p = 0.2$ is much larger than that in our exceptionally stable glass with $T_p = 0.062$. Recent studies^{31,32,47} have indicated that sound attenuation in the harmonic approximation may be proportional to the density of quasi-localized modes, and that the density of these quasi-localized modes decreases rapidly with increasing stability^{41,48}. These modes may also be responsible for finite temperature sound attenuation. It has also been found that the distribution of the local elastic constants narrows with increasing stability⁴⁹, and this may also give rise to the difference in the stability dependence of sound attenuation.

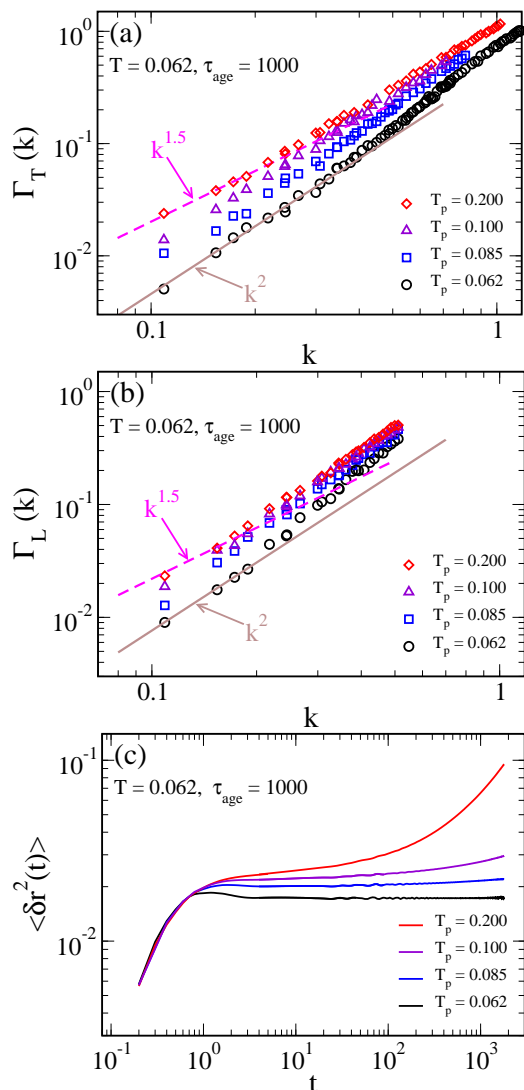


FIG. 5: Wavevector k dependence of $\Gamma_T(k)$ (a) and $\Gamma_L(k)$ (b) in glasses with the same temperature $T = 0.062$ and aging time $\tau_{\text{age}} = 1000$ for different parent temperatures T_p . The dashed and solid lines correspond to $k^{1.5}$ and k^2 , respectively. (c) The mean-squared displacement $\langle \delta r^2(t) \rangle$ for glasses shown in (a) and (b).

V. CONCLUSIONS

We examined finite temperature sound attenuation in glasses over a wide range of stabilities, with the most stable glasses having stability comparable to that of experimental glasses. For glasses undergoing aging, sound attenuation $\Gamma_\lambda(k)$ scales with wavevector k as $k^{1.5}$. We identify simulations where this aging effect is present by the appearance of an upturn in the mean square displacement. When we see no upturn in the mean square displacement, then $\Gamma_\lambda(k) \sim k^2$ for small wavevectors. As the glass's stability increases, through aging or by using a different preparation protocol, sound attenuation decreases. The decrease is most significant at small

wavevectors.

For our most stable glasses at finite temperatures, we were able to clearly observe the three scaling regimes discussed by Baldi *et al.*¹², the small and large wavevector quadratic scaling and the intermediate wavevector quartic scaling. With increasing temperature, the small wavevector sound attenuation increases significantly, while the large wavevector attenuation remains nearly unchanged. We find that the wavevector (frequency) where thermal effects begin to become significant scales as $T^{0.22}$. It would be interesting to see if this scaling is universal or depends on the specifics of the glass.

We determined that the coefficient describing the small wavevector quadratic scaling increases as approximately $T^{1/2}$. This temperature dependence was predicted by Schirmacher²⁷ and observed in simulations of Mizuno and Mossa^{37,38}. However, according to Schirmacher's theory it should occur for a system close to an elastic instability where the small wavevector scaling of sound attenuation is $k^{1.5}$ instead of the observed k^2 .

Future work needs to examine the role of quasi-localized modes and variations of local elasticity in sound attenuation. Mizuno determined that the increase in attenuation with temperature correlated with an increase in the width of the distribution of local elastic constants³⁸. Shakerpoor *et al.*⁴⁹ found that the variation of the local elastic constants decreases with increasing stability for the glass former examined in this work, and this decrease also correlates with the decrease in sound attenuation reported by Wang *et al.*³².

It has been argued by Schirmacher *et al.*⁴⁷ on the basis of fluctuating elasticity theory that sound attenuation is related to the excess density of states $D_{ex}(\omega)$, which corresponds to the density of quasi-localized modes in recent work^{41,50,51}. Recent studies^{41,48,50-59} within the harmonic approximation show that $D_{ex}(\omega)$ scales universally with ω^4 at low ω and that $D_{ex}(\omega) \sim \Gamma(\omega)^{32}$. Future work should examine the connection between the change of sound attenuation and $D_{ex}(\omega)$, specifically whether the anharmonicity also alters the ω^4 scaling of $D_{ex}(\omega)$ and the connection to the anharmonic properties of quasi-localized modes^{60,61}.

Conflicts of interest

There are no conflicts to declare.

Acknowledgements

We thank H. Mizuno and his coworkers for kind correspondence regarding some results of this work. This work was supported by NSF Grants DMR-1608086 (E.F. and G.S.) and CHE-1800282 (E.F. and G.S.), and the Start-up Fund from Anhui University S020318001/02

(L.W.). We also acknowledge Beijing Computational Science Research Center and the High-Performance Com-

puting Platform of Anhui University for providing computing resources.

-
- ¹ M. P. Zaitlin and A. C. Anderson, *Phys. Rev. B: Solid State*, 1975, **12**, 4475-4486.
- ² R. O. Pohl, X. Liu and E. Thompson, *Rev. Mod. Phys.*, 2002, **74**, 991-1013.
- ³ R. C. Zeller and R. O. Pohl, *Phys. Rev. B*, 1971, **4**, 2029-2041.
- ⁴ W. A. Phillips, *J. Low Temp. Phys.* 1972, **7**, 351-360.
- ⁵ P. W. Anderson, B. I. Halperin and C. M. Varma, *Philos. Mag.*, 1972, **25**, 1-9.
- ⁶ V. Lubchenko and P. G. Wolynes, *Proc. Natl. Acad. Sci. USA*, 2003, **100** 1515-1518.
- ⁷ V. Lubchenko and P. G. Wolynes, *Phys. Rev. Lett.*, 2001, **87**, 195901.
- ⁸ V. Lubchenko, *Adv. Phys.: X*, 2018, **3**, 1510296.
- ⁹ B. Rufflé, G. Guimbretière, E. Courtens, R. Vacher and G. Monaco, *Phys. Rev. Lett.*, 2006, **96**, 045502.
- ¹⁰ G. Monaco and V. M. Giordano, *Proc. Natl. Acad. Sci. USA*, 2009, **106**, 3659-3663.
- ¹¹ G. Baldi, V. M. Giordano, G. Monaco and B. Ruta, *Phys. Rev. Lett.*, 2010, **104**, 195501.
- ¹² G. Baldi, V. M. Giordano, B. Ruta, R. Dal Maschio, A. Fontana and G. Monaco, *Phys. Rev. Lett.*, 2014, **112**, 125502.
- ¹³ G. Baldi, M. Zanatta, E. Gilioli, V. Milman, K. Refson, B. Wehinger, B. Winkler, A. Fontana and G. Monaco, *Phys. Rev. Lett.*, 2013, **110**, 185503.
- ¹⁴ B. Ruta, G. Baldi, F. Scarponi, D. Fioretto, V. M. Giordano and G. Monaco, *J. Chem. Phys.*, 2012, **137**, 214502.
- ¹⁵ C. Masciovecchio, G. Baldi, S. Caponi, L. Comez, S. Di Fonzo, D. Fioretto, A. Fontana, A. Gessini, S. C. Santucci, F. Sette, G. Vilianni, P. Vilmercati and G. Ruocco, *Phys. Rev. Lett.*, 2006, **97**, 035501.
- ¹⁶ C. Masciovecchio, A. Gessini, S. Di Fonzo, L. Comez and S. C. Santucci, D. Fioretto, *Phys. Rev. Lett.*, 2004, **92**, 247401.
- ¹⁷ P. Benassi, S. Caponi, R. Eramo, A. Fontana, A. Giugni, M. Nardone, M. Sampoli and G. Vilianni, *Phys. Rev. B*, 2005, **71**, 172201.
- ¹⁸ T. Scopigno, J.-B. Suck, R. Angelini, F. Albergamo and G. Ruocco, *Phys. Rev. Lett.*, 2006, **96**, 135501.
- ¹⁹ A. Devos, M. Foret, S. Ayrinhac, P. Emery and B. Rufflé, *Phys. Rev. B*, 2008, **77**, 100201(R).
- ²⁰ C. Zener, *Phys. Rev.*, 1938, **53**, 90-99.
- ²¹ R. Lifshitz and M. L. Roukes, *Phys. Rev. B*, 2000, **61**, 5600-5609.
- ²² S.K. De and N. R. Aluru, *Phys. Rev. B*, 2006, **74**, 144305.
- ²³ A. Akhiezer, *J. Phys.*, 1939, **1**, 277.
- ²⁴ H. J. Maris, *In Physical Acoustics*, edited by W. P. Mason and R. N. Thurston, Academic Press, New York, 1971, **8**, 279.
- ²⁵ C. Tomaras, B. Schmid and W. Schirmacher, *Phys. Rev. B*, 2010, **81**, 104206.
- ²⁶ C. Ferrante, E. Pontecorvo, G. Cerullo, A. Chiasera, G. Ruocco, W. Schirmacher and T. Scopigno, *Nat. Commun.*, 2013, **4**, 1793.
- ²⁷ A. Marruzzo, S. Köhler, A. Fratolocci, G. Ruocco, and W. Schirmacher, *Eur. Phys. J. Spec. Top.*, 2013, **216**, 83-93.
- ²⁸ C. Tomaras, B. Schmid and W. Schirmacher, *Phys. Rev. B*, 2010, **81**, 104206.
- ²⁹ C. Caroli and A. Lemaître, *Phys. Rev. Lett.*, 2019, **123**, 055501.
- ³⁰ H. Mizuno and A. Ikeda, *Phys. Rev. E*, 2018, **98**, 062612.
- ³¹ A. Moriel, G. Kapteijns, C. Rainone, J. Zylberg, E. Lerner and E. Bouchbinder, *J. Chem. Phys.*, 2019, **151**, 104503.
- ³² L. Wang, L. Berthier, E. Flenner, P. Guan and G. Szamel, *Soft Matter*, 2019, **15**, 7018-7025.
- ³³ S. Gelin, H. Tanaka and A. Lemaitre, *Nat. Mater.*, 2016, **15**, 1177-1181.
- ³⁴ L. Berthier, D. Coslovich, A. Ninarello and M. Ozawa, *Phys. Rev. Lett.*, 2016, **116**, 238002.
- ³⁵ A. Ninarello, L. Berthier and D. Coslovich, *Phys. Rev. X*, 2017, **7**, 021039.
- ³⁶ R. Busselez, T. Pezeril and V. E. Gusev, *J. Chem. Phys.*, 2014, **140**, 234505.
- ³⁷ H. Mizuno and S. Mossa, *Condens. Matter Phys.*, 2019, **22**, 43604.
- ³⁸ H. Mizuno, G. Ruocco and S. Mossa, 2019, arXiv:1905.10235.
- ³⁹ S. F. Swallen, K. L. Kearns, M. K. Mapes, Y. S. Kim, R. J. McMahon, M. D. Ediger, T. Wu, L. Yu and S. Satija, *Science*, 2007, **315**, 353-356.
- ⁴⁰ L. Berthier, P. Charbonneau, E. Flenner and F. Zamponi, *Phys. Rev. Lett.*, 2017, **119**, 188002.
- ⁴¹ L. Wang, A. Ninarello, P. Guan, L. Berthier, G. Szamel and E. Flenner, *Nat. Commun.*, 2019, **10**, 26.
- ⁴² E. Bitzek, P. Koskinen, F. Gähler, M. Moseler and P. Gumbsch, *Phys. Rev. Lett.*, 2006, **97**, 170201.
- ⁴³ S. Plimpton, *J. Comput. Phys.*, 1995, **119**, 1-19.
- ⁴⁴ <https://lammps.sandia.gov/>.
- ⁴⁵ E. Bouchbinder and E. Lerner, *New J. Phys.*, 2018, **20**, 073022.
- ⁴⁶ G. Monaco and S. Mossa, *Proc. Natl. Acad. Sci. USA*, 2009, **106**, 16097-16912.
- ⁴⁷ W. Schirmacher, G. Ruocco and T. Scopigno, *Phys. Rev. Lett.*, 2007, **98**, 025501.
- ⁴⁸ C. Rainone, E. Bouchbinder and E. Lerner, *Proc. Natl. Acad. Sci. USA*, 2020, **117**, 5228-5234.
- ⁴⁹ A. Shakerpoor, E. Flenner and G. Szamel, *Soft Matter*, 2020, **16**, 914-920.
- ⁵⁰ E. Lerner, G. Düring and E. Bouchbinder, *Phys. Rev. Lett.*, 2016, **117**, 035501.
- ⁵¹ H. Mizuno, H. Shiba and A. Ikeda, *Proc. Natl. Acad. Sci. USA*, 2017, **114**, E9767-E9774.
- ⁵² U. Buchenau, Yu. M. Galperin, V. L. Gurevich, D. A. Parshin, M. A. Ramos, H. R. Schober, *Phys. Rev. B*, 1992, **46**, 2798-2808.
- ⁵³ H. R. Schober and C. Oligschleger, *Phys. Rev. B*, 1996, **53**, 11469-11480.
- ⁵⁴ V. L. Gurevich, D. A. Parshin and H. R. Schober, *Phys. Rev. B*, 2003, **67**, 094203.
- ⁵⁵ G. Kapteijns, E. Bouchbinder and E. Lerner, *Phys. Rev. Lett.*, 2018, **121**, 055501.
- ⁵⁶ L. Angelani, M. Paoluzzi, G. Parisi and G. Ruocco, *Proc. Natl. Acad. Sci. USA*, 2018, **115**, 8700-8704.

- ⁵⁷ H. Ikeda, *Phys. Rev. E*, 2019, **99**, 050901(R).
- ⁵⁸ F. P. Benetti, G. Parisi, F. Pietracaprina and G. Sicuro, *Phys. Rev. E*, 2018, **97**, 062157.
- ⁵⁹ E. M. Stanifer, P. K. Morse, A. A. Middleton and M. L. Manning, *Phys. Rev. E*, 2018, **98**, 042908.
- ⁶⁰ H. Mizuno, M. Shimada and A. Ikeda, 2019, arXiv:1911.07211.
- ⁶¹ N. Xu, V. Vitelli, A. J. Liu and S. R. Nagel, *Europhys. Lett.*, 2010, **90**, 56001.